Supporting Information

Identifying Hexagonal 2D Planar Electrocatalysts with Strong OCHO* Binding for Selective CO_2 Reduction

Yuefeng Zhang [1], Tianyi Wang [3], Fei Wang [4], Huiling Zheng [5], Zhiyuan Zeng [1,2*], and Hao Li [3*]

[1] Department of Materials Science and Engineering, and State Key Laboratory of Marine Pollution, City University of Hong Kong, 83 Tat Chee Avenue, Kowloon, Hong Kong 999077, China.

[2] Shenzhen Research Institute, City University of Hong Kong, Shenzhen 518057, China

[3] Advanced Institute for Materials Research (WPI-AIMR), Tohoku University, Sendai 980-8577, Japan.

[4] Key Laboratory of Special Functional Materials for Ecological Environment and Information (Hebei University of Technology), Ministry of Education, Tianjin, 300130, China

[5] State Key Laboratory of Clean and Efficient Coal Utilization, Taiyuan University of Technology, Taiyuan 030024, China

[*] Correspondence should be addressed to:

zhiyzeng@cityu.edu.hk (Z.Z.)

li.hao.b8@tohoku.ac.jp (H.L.)

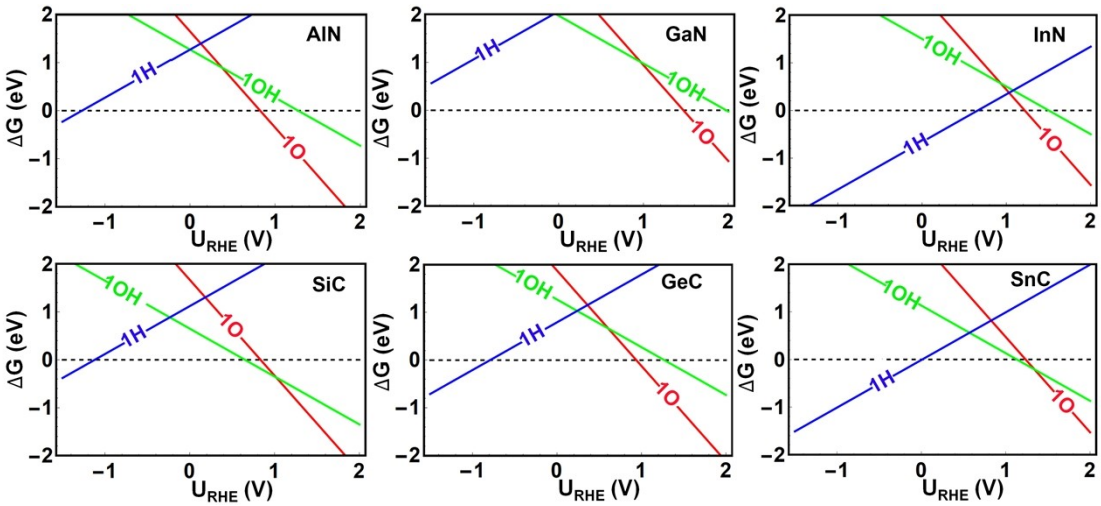

Fig. S1. The calculated 1D Pourbaix diagrams of the 2D monolayer systems at pH = 0.

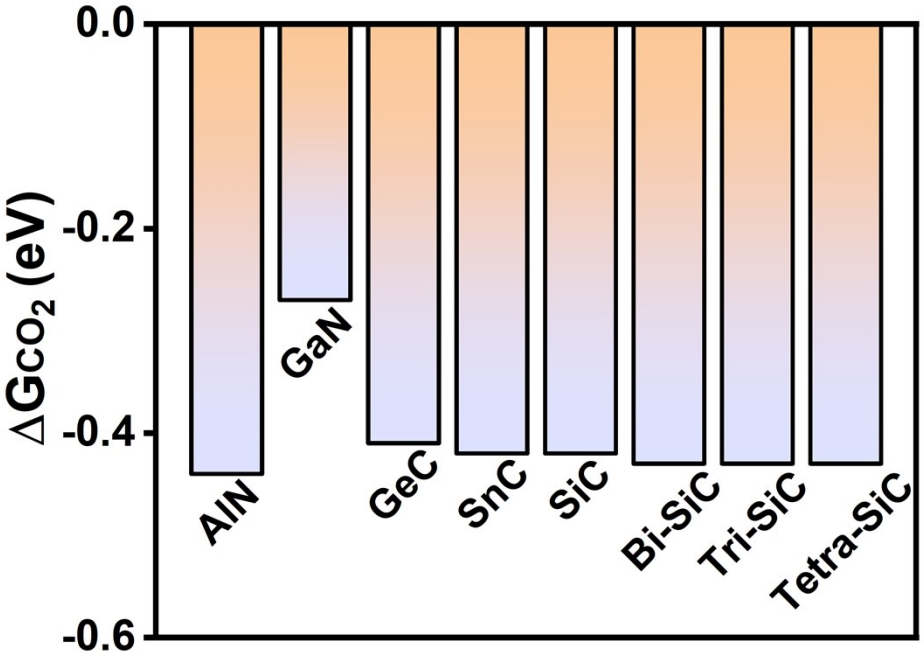

Fig. S2. Gibbs free energies of CO_2 adsorption at the 2D catalysts.

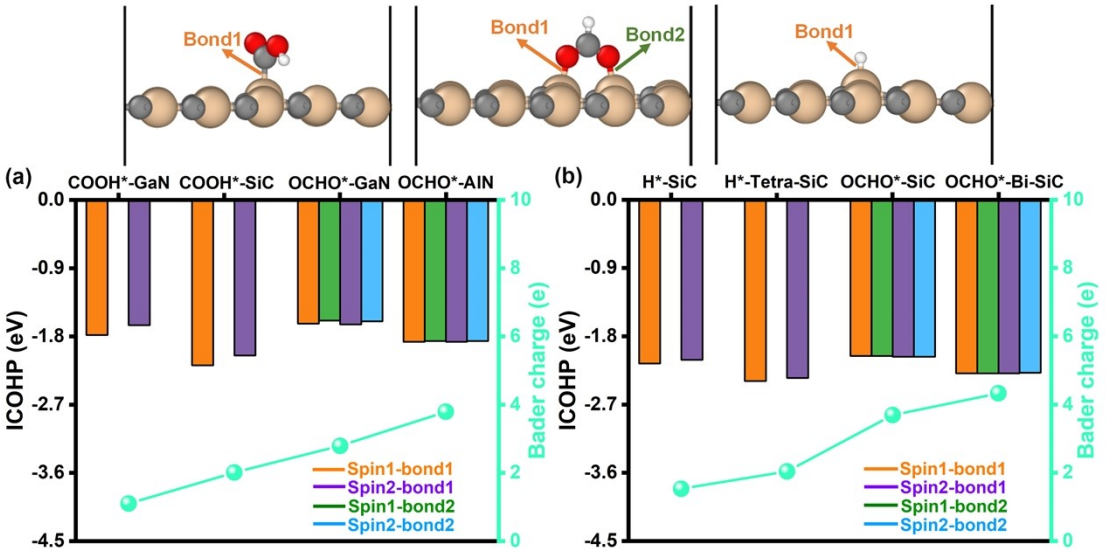

Fig. S3. The integrated crystal orbital Hamilton population (ICOHP) and charge variation for (a) COOH* on GaN and SiC, and OCHO* on GaN and AlN; (b) H* on SiC and Tetra-SiC and OCHO* on SiC and Bi-SiC, where positive values represent electrons lost.

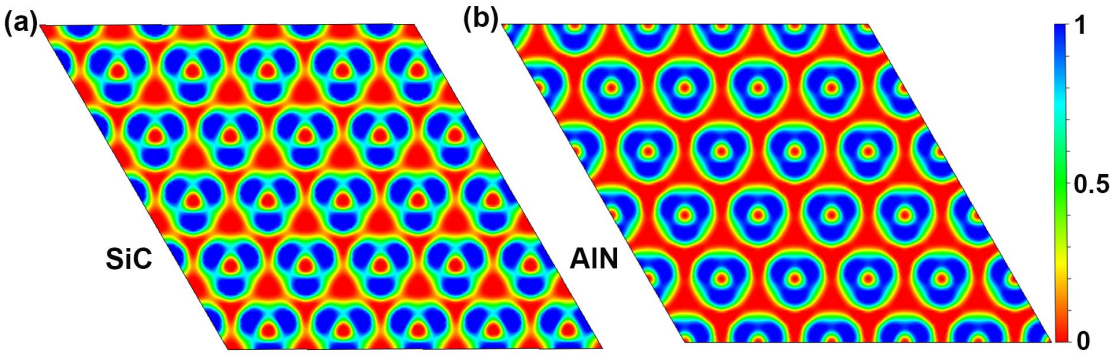

Fig. S4. Electron localization functions of (a) SiC and (b) AlN.

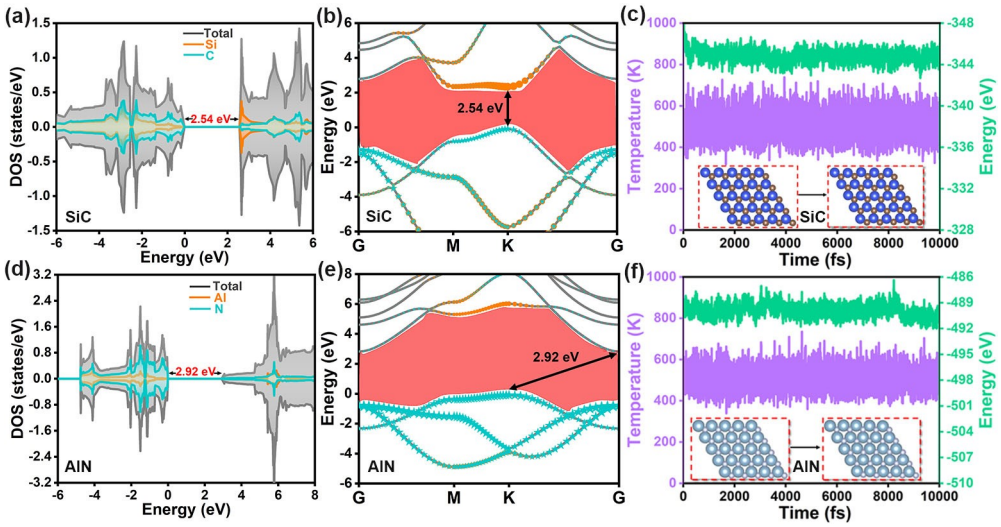

Fig. S5. Projected density of states of (a) SiC and (d) AlN. Projected band structure of (b) SiC and (e) AlN. *Ab initio* molecular dynamics (AIMD) simulations under 500 K at (c) SiC and (f) AlN.

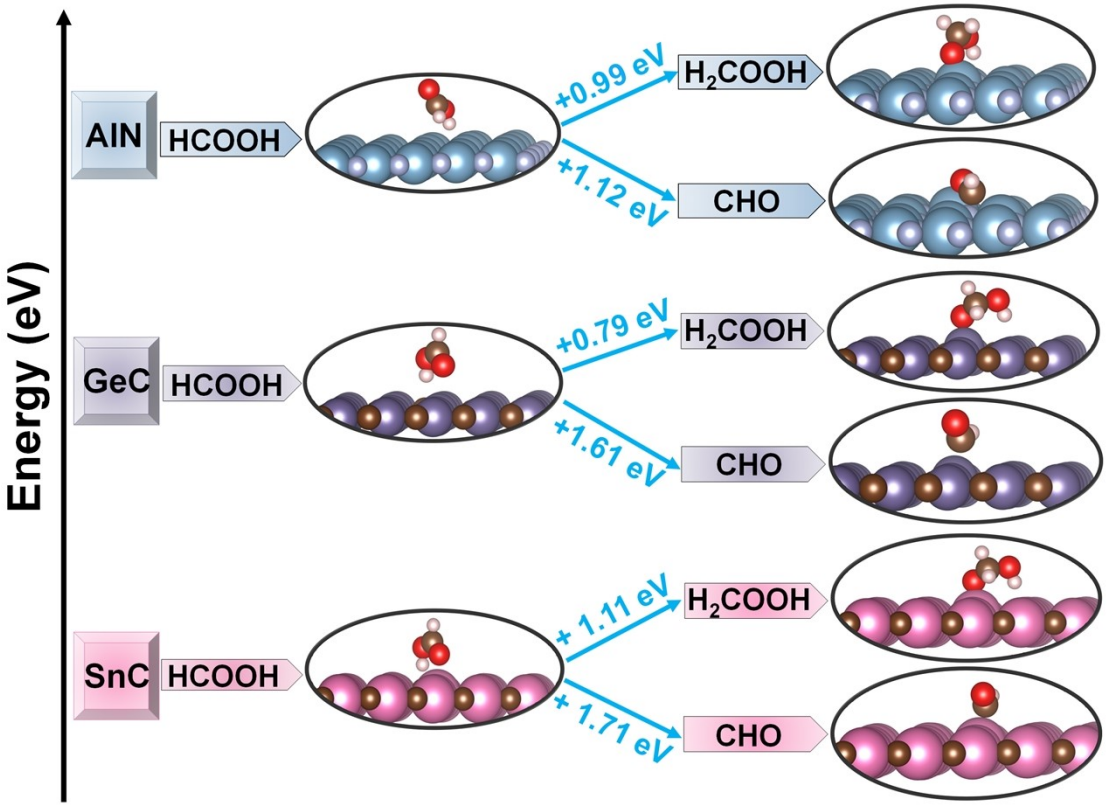

Fig. S6. Free energy profiles of the further protonation of HCOOH* and the optimized geometric structures of AlN, GeC, and SnC. Al, Ge, Sn, H, O, C, and N are denoted by sky blue, dark purple, bright pink, light pink, red, gray, and light blue spheres, respectively.

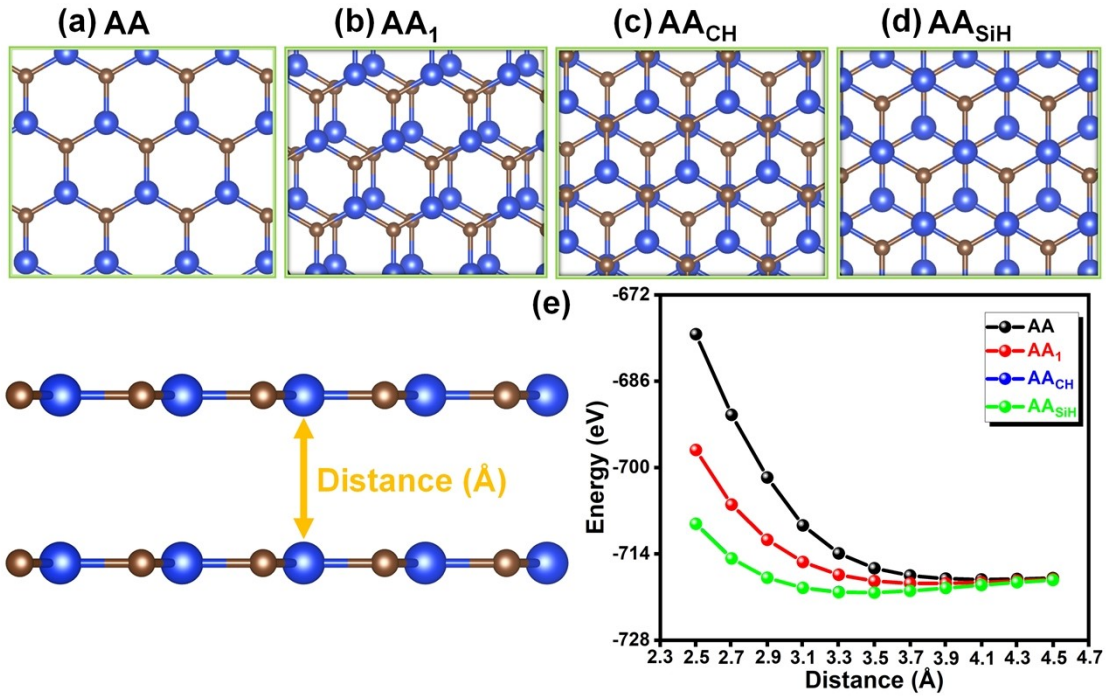

Fig. S7 Possible stacking modes of the bi-SiC model: (a) AA, (b) AA1, (c) AA_{CH}, and (d) AA_{SiH}. (e)Single point energy as a function of interlayer distance for bi-SiC. Si and C elements are presented by blue and gray balls, respectively.

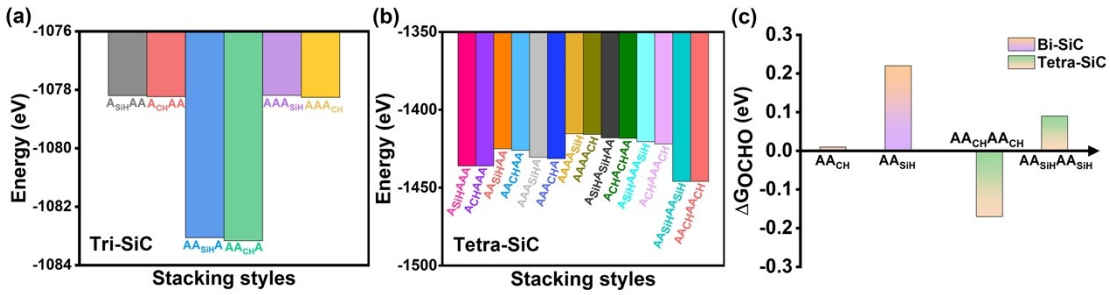

Fig. S8 Variation of single point energies brought about by the various stacking styles of (a) tri-SiC and (b) tetra-SiC models. (c) Gibbs free energies of OCHO* adsorption on AA_{CH}, AA_{SiH}, $AA_{CH}AA_{CH}$, and $AA_{SiH}AA_{SiH}$.

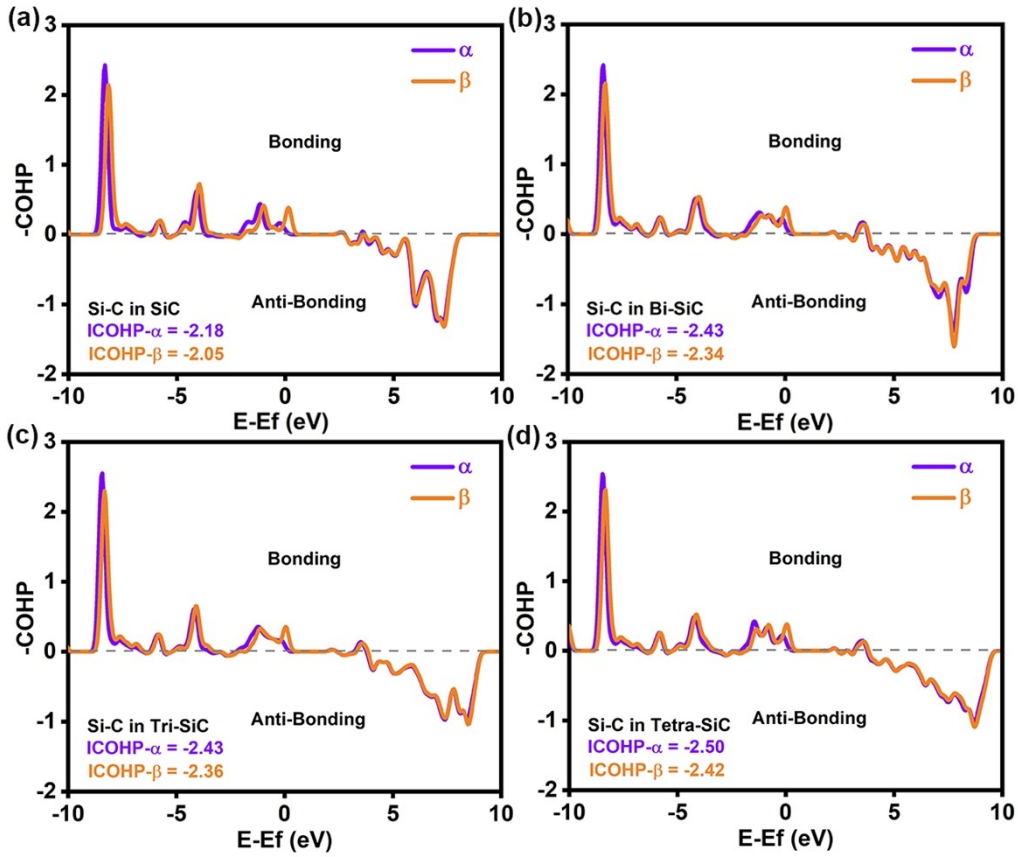

Fig. S9. COHP for the C in COOH* bonded to the SiC (a), Bi-SiC (b), Tri-SiC (c), Tetra-SiC (d). The bonding and antibonding states are shown on the up and the down of the horizontal zero line. α and β represent spin up and down, respectively.